Solving complex photocycle kinetics

Theory and direct method

John F. Nagle
Departments of Biological Sciences and Physics, Carnegie Mellon University, Pittsburgh, Pennsylvania 15213 USA

ABSTRACT A direct nonlinear least squares method is described that obtains the true kinetic rate constants and the temperature-independent spectra of n intermediates from spectroscopic data taken in the visible at three or more temperatures. A theoretical analysis, which is independent of implementation of the direct method, proves that well determined local solutions are not possible for fewer than three temperatures. This analysis also proves that measurements at more than n wavelengths are redundant, although the direct method indicates that convergence is faster if $n + m$ wavelengths are measured, where m is of order one. This suggests that measurements should concentrate on high precision for a few measuring wavelengths, rather than lower precision for many wavelengths. Globally, false solutions occur, and the ability to reject these depends upon the precision of the data, as shown by explicit example. An optimized way to analyze vibrational spectroscopic data is also presented. Such data yield unique results, which are comparably accurate to those obtained from data taken in the visible with comparable noise. It is discussed how use of both kinds of data is advantageous if the data taken in the visible are significantly less noisy.

1. INTRODUCTION

Many important processes in the biological sciences are rather complex, with kinetics involving several intermediate steps and with branching pathways and backreactions. The particular process that motivates this paper is the kinetic photocycle of bacteriorhodopsin (bR) in the purple membrane of *Halobacterium halobium,* but the analysis of this problem should have wider applicability.

A favorite way to study such processes is to measure their absorbance changes in the visible wavelength range, which can be done with high signal to noise (18). The complication with this experimental approach is that the spectra of the intermediates are broad, so that the measured absorbance change is generally due to a mixture of several different intermediates, as well as the problem that the intermediates overlap in time so that there is no time at which the signal is due to just one intermediate. The problem of deconvoluting signals of this type into a workable kinetic model is a nontrivial one.

In the case of bR a detailed analysis has been performed showing how the number of intermediates can be obtained by spectroscopy in the visible range (18). Seven intermediates have been deduced in the time range after 1 μs and the apparent rate constants and the decay amplitudes were found to satisfactory accuracy (18). That paper represented the first part of a two part process of determining the photocycle. This paper focusses upon the concluding part which includes the true rate constants and the spectra of the intermediates. No direct method has existed for the determination of this concluding part. Instead, various kinetic models have been proposed (8, 16, 2, 5, 7, 17), based on the interpretation of various data. Some of these models have then been tested, tediously and one by one, against the best quantitative data (11, 13, 9). One purpose of this paper is to describe a direct method for determining photocycles from spectroscopic data in the visible wavelength range.

A second purpose of this paper is to provide a theoretical analysis of the kind and quality of data required to solve these kinetic problems. One decision that must be made experimentally is whether to concentrate on very good statistics for a few measuring wavelengths or to concentrate on measuring at many wavelengths with perhaps a sacrifice in statistics. Another question is whether data of sufficient precision can be obtained to discriminate against false solutions that may occur in complex nonlinear least squares problems.

A second way to study such processes is to measure their vibrational spectra. In the case of bacteriorhodopsin raw resonance Raman data have recently been used to obtain the time course of the concentration of the intermediates (1). The third purpose of this paper is to present an optimized way to obtain the photocycle from such concentration data.

It may be mentioned that because resonance Raman and visible spectroscopy both detect changes in the retinal chromophore, the photocycle detected by both methods ought to be the same. Other kinetic properties, such as those measured electrically (14) or by UV

0006-3495/91/02/476/12 $2.00

difference spectroscopy (15), may then be compared to the photocycle of the chromophore to determine differences in the kinetics of the different parts of bacteriorhodopsin.

2. MATHEMATICAL FORMULATION OF THE PROBLEM

Although the problem of obtaining the photocycle from spectroscopic data in the visible is different from the problem of obtaining it from vibrational data, it will be convenient in this section to define the two problems with a common mathematical notation.

In this paper it will be assumed that the kinetic process is initiated at time $t = 0$, such as by a fast laser flash. The unexcited state of the system will be designated as state 0. The excited portion of the sample will be assumed to go into a single intermediate, designated by $i = 1$, at $t = 0$. Subsequently, state 1 decays to the unexcited state 0 and this decay involves other intermediates $i = 2, \ldots, n$. Designating the amount (or probability) of excited material being in state i at time t by $p_i(t)$, these initial conditions are expressed as $p_1(0) = 1$ and $p_i(0) = 0$ for $i \neq 1$. (However, other initial conditions may also be dealt with.)

For bR at temperatures above 273 K there is evidence that the thermal transitions between intermediates are first order (18), in which case the kinetic development of the system is given by the coupled first-order differential equations:

$$dp_i(t)/dt = \sum_{j=0,n} K_{ij} p_j(t) \text{ for } i = 0, \ldots, n,$$
$$\text{where } K_{ii} = -\sum_{m=0,n} K_{mi}, m \neq i, \quad (1)$$

where for $j \neq i$, K_{ij} is the first-order rate constant for decay of intermediate j to intermediate i and for $j = i$, K_{ii} is the negative of the sum of the rate constants from intermediate i to all other intermediates. It will also be assumed in this paper that the final state is the same as the initial state 0, so that $p_0(\infty) = 1$ and $p_i(\infty) = 0$ for $i \neq 0$. This requires that there be no backreactions from state 0, so $K_{i,0} = 0$ for all i. (This is not an essential assumption for the methods to be described in this paper, which could equally well deal with the case when the final state at $t = \infty$ is a mixture of the intermediates.) It is convenient to use matrix and vector notation, in which Eq. 1 becomes

$$d\mathbf{p}(t)/dt = \mathbf{K}\mathbf{p}(t), \quad (2)$$

where $\mathbf{K}$ is the $n + 1$ by $n + 1$ matrix with entries K_{ij} and $\mathbf{p}(t)$ is the vector $[p_1(t), p_2(t), \ldots, p_n(t), p_0(t)]$. (The $[n + 1]$st row of $\mathbf{K}$ consists of the rates $K_{0,i}$. The $[n + 1]$st column consists of zeros when no backreactions from 0 are allowed, so this trivial column will not be shown subsequently in this paper.) The $\mathbf{K}$ matrix contains the true rate constants for the process. It is the basic kinetic description that one wishes to obtain from experiment.

The true rate constants K_{ij} must satisfy the law of detailed balance (12), for example

$$K_{ab}K_{bc}K_{ca} = K_{ac}K_{cb}K_{ba}, \quad (3)$$

where, of course, the cycles may be longer than the three-cycle, *abc*. Therefore, not all the K_{ij} are independent quantities. The maximum number N_K of independent K's when no backreactions from state 0 are allowed is $[n(n + 3) - 2]/2$. (N_K increases by 1 when backreactions from state 0 are allowed. Also, N_K may be smaller than the maximum if some rates are required to be identically zero.) An important consequence of detailed balance is that the time dependence of each intermediate is a sum of real exponentials

$$p_i(t) = \sum_{j=1,n} C_{ji} \exp(-tk^*_j) \text{ or } \mathbf{p}(t) = \exp(-t\mathbf{k}^*)\mathbf{C}. \quad (4)$$

The rate constants $\mathbf{k}^* = \{k^*_j\}$ are called the apparent rate constants; they are generally non-trivially related to the true rate constants as are the coefficients C_{ji} in the $\mathbf{C}$ matrix (Eq. 4 requires minor modification if some of the k^*_j are accidentally degenerate.) Note that the upper limit in the sum is precisely n where there are n intermediates.

Given values for the true rate constants it is routine to solve Eq. 2 to obtain the apparent rate constants $\mathbf{k}^*$ and the $\mathbf{C}$ on the right-hand side of Eq. 4 and thereby obtain $\mathbf{p}(t)$. The analysis uses standard Laplace transform theory. The procedure has been translated into a computer program which requires 0.36 s microvax II cpu time for $n = 3$ intermediates and $s = 10$ wavelengths and this time increases to 0.55 s for $n = 5$. Given numerical values for some property of the intermediates, such as the spectra in the visible range for bacteriorhodopsin, it is therefore very easy to calculate measurable quantities, such as the visible absorbance changes given by

$$\Delta A(t, \lambda) = \sum_i p_i(t)\epsilon_i(\lambda) \equiv \mathbf{p}(t) \cdot \boldsymbol{\epsilon}(\lambda), \quad (5)$$

where $\boldsymbol{\epsilon}(\lambda) = \{\epsilon_i(\lambda)\}$ are the relative spectra of the intermediates, i.e., $\epsilon_i(\lambda)$ is the spectrum of intermediate i minus the spectrum of bR.

From Eq. 4, the absorbance changes $\Delta A(t, \lambda)$ also can be written as a sum of exponentials

$$\Delta A(t, \lambda) = \sum_{j=1,n} \exp(-tk^*_j) b_j(\lambda)$$
$$\equiv \exp(-t\mathbf{k}^*) \cdot \mathbf{b}(\lambda). \quad (6)$$

Using Eq. 4 in Eq. 5 and equating the coefficients of $\exp(-tk_j^*)$ for each j with those in Eq. 6 yields

$$b_j(\lambda) = \sum_{j=1,n} C_{mj}\epsilon_j(\lambda) \text{ or } \mathbf{b}(\lambda) = \mathbf{C}\boldsymbol{\epsilon}(\lambda). \quad (7)$$

Extracting the apparent rate constants $\mathbf{k}^*$ and the amplitudes, $\mathbf{b}(\lambda)$, from the data $\Delta A(t, \lambda)$ is accomplished by the Variable Projection (VARP) program of Golub and Leveque (4) which fits the data for all t and λ globally to the same apparent rate constants. This is now a routine procedure and was central to obtaining the number of intermediates n for the bR photocycle (18). However, this is only a first step in determining the photocycle from spectroscopic data in the visible.

The problem in analyzing spectroscopic data for visible wavelengths, $\Delta A(t, \lambda)$, is to invert Eq. 5 to obtain the spectral ϵ and the true rate constants $\mathbf{K}$. It may first be remarked that in cases where the spectra of all the intermediates are known, then Eq. 5 may be solved easily for the $\mathbf{p}(t)$ which would make this the same as the problem of analyzing vibrational data. As we shall see in section 4 the analysis of this problem is straightforward. Generally, however, one does not know the visible spectra and so the problem of solving the photocycle from spectroscopy measurements in the visible is more challenging.

3. THEORY FOR DATA IN THE VISIBLE

Necessary and sufficient conditions for the visible spectroscopy problem to be solvable in principle will be discussed in this section. The importance of this theoretical analysis is emphasized by the fact that the problem as posed at the end of the previous section is generally an indeterminate problem. This can be seen by counting unknowns and comparing to the amount of information in the data. Since the data have the representation shown in Eq. 6, they can be completely described by $\mathbf{b}(\lambda)$ and the $\mathbf{k}^*$, as well as by residuals which describe the noise and therefore contain no real information if there are no systematic errors. The amount of information can be quantified by the number, n, of $\mathbf{k}^*$ plus the number, ns, of amplitudes $\mathbf{b}(\lambda)$, where s is the number of wavelengths λ measured. The number of unknowns is the number, ns, of extinctions $\epsilon(\lambda)$ required to describe the spectra at the measured wavelengths plus the number of independent true rate constants, $N_K = [n(n + 3) - 2]/2$. Therefore, the number of unknowns exceeds the amount of information in the data, because N_K exceeds n except for the trivial $n = 1$ case.

Generally, an infinite number of values for the $\mathbf{K}$ matrix give the same $\mathbf{k}^*$ and $\mathbf{b}$ and therefore fit the data equally well. Note, however, that each different set of true rate constants that fits the data also gives different spectra $\boldsymbol{\epsilon}(\lambda)$. It might also be emphasized that the reverse is true, and this has important implications for attempting to do the analysis by first guessing the spectra (17). In Fig. 1 are shown the spectra of the intermediates of a model with three intermediates from which data were calculated assuming a kinetic model with both forward and backreactions K ↔ L ↔ M → bR. When a reasonable guess for the spectra is made by changing the spectra of L and M to the dashed lines, the fit is equally good (perfect for noiseless data), but the derived model has a branch L → bR and no backreactions. Changing M further to the dot-dash line yields an unbranched, unidirectional model which again fits the data perfectly.

As described in the preceding two paragraphs the solution only becomes determinate if the number of true rate constants is limited to n, which requires a unidirectional, unbranched kinetic model. (Even then, permutation of rate constants leads to a quasi-indeterminacy [11].) However, when unidirectional unbranched kinetic models are fit to bR data taken at two different temperatures, the resulting calculated spectra vary too rapidly with temperature to be believable (11) in view of the rather small changes in the spectra of various chromophores in comparable temperature ranges. This is a strong criterion to test proposed kinetic models, including models more complicated than unidirectional, unbranched models (13).

In this paper the criterion of the invariance with temperature of the spectra $\boldsymbol{\epsilon}$ will supply additional information that makes determinate the problem of solving kinetic photocycles. The idea is that measurements at N_T temperatures still have ns unknown $\boldsymbol{\epsilon}$, but the number of known amplitudes $\mathbf{b}(\lambda)$ increases to $N_T(ns)$. Before completing the comparison of knowns to

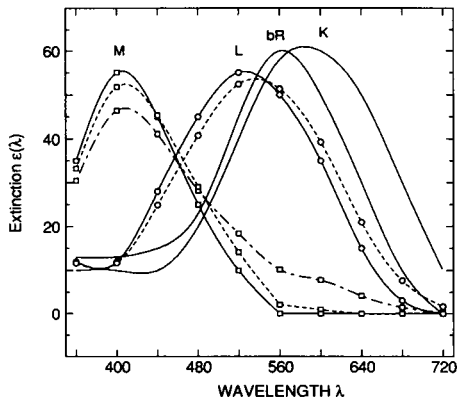

FIGURE 1 An example of three different sets of spectra that yield three distinct kinetic models when applied to the same kinetic data.

unknowns, it is necessary first to discuss the temperature dependence of the K_{ij}.

It is usual to suppose that the true rate constant K_{ij} for the individual decay from j to i has an Arrhenius temperature dependence, such as

$$\begin{aligned} K_{ij}(T) &= f_0 \exp(-\Delta F_{ij}/kT) \\ &= f_0 \exp(\Delta S_{ij}/k - \Delta E_{ij}/kT) \\ &\equiv f_{ij} \exp(-\Delta E_{ij}/kT), \end{aligned} \tag{8}$$

where ΔF_{ij} is the free energy of activation for the $j \rightarrow i$ decay which can be decomposed into entropic $T\Delta S_{ij}$ and energetic (or enthalpic) ΔE_{ij} parts. The factor f_0 equals kT/h in Eyring's absolute rate theory (3). In the examples in this paper f_0 will be independent of temperature. Either case can be treated equally easily, and both should be tried when analyzing data. The backreaction $i \rightarrow j$ obeys a similar relation to Eq. 8 and

$$\Delta E_{ji} = \Delta E_{ij} + E_j - E_i, \tag{9}$$

where E_m is the energy of state m. If i and j were pure nondegenerate quantum states, then ΔS_{ij} would equal ΔS_{ji} and both would represent the entropy of the activated complex. But for intermediate states of complex biological processes, it seems prudent to allow that the degeneracies of intermediates i and j may be vastly different, so

$$\Delta S_{ji} = \Delta S_{ij} + S_j - S_i \tag{10}$$

and f_{ij} need not equal f_{ji} in Eq. 8. Eqs. 9 and 10 lead directly to the detailed balance Eq. 3. Additionally, Eq. 8 shows that two parameters, f_{ij} and ΔE_{ij}, determine each of the N_K independent rate constants K_{ij} for all temperatures. Therefore, if the temperature dependence obeys an Arrhenius form, the number of unknowns in the $\mathbf{K}(T)$ matrices is only $2N_K$ for all temperatures, and the examples in this paper will assume this. However, it should be emphasized that it is not necessary to make this assumption, although then the number of unknowns in the $\mathbf{K}(T)$ matrices increases to $N_T N_K$. If the Arrhenius assumption is not made, then the solution of the kinetic model allows the determination of the temperature dependence of the true rate constants.

Let us now resume the counting of knowns and unknowns to determine whether the visible spectroscopic problem can be solved. Before beginning the main work, however, two obvious points should be mentioned. First, it is well-known that the global uniqueness of solutions to nonlinear problems cannot be guaranteed by counting knowns and unknowns, but it is still useful in determining local uniqueness. (Local uniqueness means the absence of local degeneracy which consists of a manifold or infinite number of equally good solutions in the solution space near one solution.) Second, various accidental degeneracies may occur that can make a generally determined problem underdetermined. For example, if the activation energies ΔE_{ij} all have the same value ΔE in Eq. 8, then there will be no new information gained at a new temperature since each $\mathbf{p}(t, T)$ will only be a function of a single homogeneous variable, $t \exp[-\Delta E/kT]$.

The next point is less obvious and more important than the points in the preceding paragraph and will occupy the remainder of this section. In counting the difference N_D between unknowns and the amount of information in the data for N_T temperatures, s wavelengths, n intermediates and $2N_K = n(n+3) - 2$ independent rate constants (assuming an Arrhenius relation), it is easy to make an error. The number of unknowns N_{un} consists first of the number of independent rate constants and to that we will temporarily add the number ns of extinctions at s measured wavelengths to obtain the estimate $N_{un} = n(n+3) - 2 + ns$. Likewise, the amount of information, N_{inf}, necessary to describe the data is the number of apparent rate constants, nN_T, plus the number of amplitudes, nsN_T, yielding the estimate $N_D = N_{inf} - N_{un} = (N_T - 1)ns + N_T n - n(n+3) + 2$. Because local uniqueness should generally be obtained when N_D becomes positive, this analysis would suggest that only $N_T = 2$ temperatures are required provided that enough wavelengths s are measured. In fact, this is not true as was discovered from numerous examples, one of which will be described in the next section.

One might be led intuitively to suspect that the analysis in the preceding paragraph is incorrect on the grounds that adding many more wavelengths necessarily means spacing the wavelengths closer together and that there would be little extra information from two wavelengths very close together if the peaks in the spectra of the intermediates are broad. While this intuitive argument is undoubtedly valid, it is irrelevant. In fact, *no* additional kinetic information is gained by measuring at more than n wavelengths due to an intrinsic linear dependency in the problem.

The analysis begins with Eq. 7 which will be written

$$\epsilon(\lambda) = \mathbf{C}^{-1}(T_1)\mathbf{b}(\lambda, T_1) = \mathbf{C}^{-1}(T_2)\mathbf{b}(\lambda, T_2) = \cdots \tag{11}$$

where the linear amplitudes $\mathbf{b}(\lambda, T)$ should be thought of as known quantities describing the data whether one determines them or not. For N_T temperatures the number of vector equations is N_T for each λ. Because each vector has n components and because λ is measured at s wavelengths, there are $N_T ns$ equations in Eq. 11. However, in an n-dimensional vector space there are only n linearly independent vectors. Therefore, once n

values of λ have been found such that the set $\{\mathbf{b}(\lambda_j, T)\}$ are linearly independent, for any subsequent λ_m, $\mathbf{b}(\lambda_m, T)$ is linearly dependent upon the set $\{\mathbf{b}(\lambda_j, T)\}$. If this linearly independent set obeys Eq. 11, then any additional linearly dependent $\mathbf{b}(\lambda_m, T)$ also automatically obeys Eq. 11. Therefore, there are only $N_T n^2$ linearly independent equations in Eq. 11, for $s \geq n$. An important consequence is that for determining the kinetic model $\mathbf{K}(T)$ there is no information to be gained by considering more than n wavelengths.

In addition to the $\mathbf{b}(\lambda)$ which are part of the equation counting in the preceding paragraph, there are also $N_T n$ apparent rates $\mathbf{k}^*(T)$ which require $N_T n$ equations involving the $\mathbf{K}(T)$ matrices, for a total of $N_T n(n + 1)$ equations. If there is an Arrhenius type relation, the number of unknowns is $2N_K + n^2$. If there is no known temperature relation, the number of unknowns is $N_T N_K + n^2$. In either case, the number of spectral unknowns to be counted is only n^2 in accordance with the linear dependency derived in the preceding paragraph. Therefore, the number of equations minus the number of unknowns, N_D, is

$$N_D = N_T n(n + 1) - n(n + 3) - 2 - n^2, \quad (12)$$

if there is an Arrhenius relation and

$$N_D = N_T n(n + 1) - (N_T/2)[n(n + 3) - 2] - n^2,$$

if there is no temperature relation.

Whether or not there is an Arrhenius-type temperature relation, it then follows easily from Eq. 12 that for kinetic processes with $n \geq 3$ intermediates there is local uniqueness, i.e., $N_D > 0$, if and only if there are three or more temperatures,

$$N_T \geq 3 \text{ for local uniqueness for } n \geq 3, \quad (13)$$

when a full set of n linearly independent wavelengths is included in the data.

4. DIRECT NONLINEAR LEAST SQUARES METHOD

Previously, no direct method has been described to implement the constraint that the visible spectra of the intermediates be invariant with temperature, and this criterion has been used simply to test kinetic models rather than to derive them. This section first describes a method to incorporate this constraint into nonlinear least squares procedures to derive kinetic models from data in the visible. Then, two direct methods to treat the vibrational problem are also described.

Let us first rewrite Eq. 5 with an explicit temperature dependence.

$$\Delta A(t, T; \lambda) = \sum_i p_i(t, T)\epsilon_i(\lambda) \equiv \mathbf{p}(t, T) \cdot \boldsymbol{\epsilon}(\lambda). \quad (14)$$

The basic idea is to fit the data simultaneously at more than one temperature as well as at all times and wavelengths. The trick in the use of nonlinear least squares procedures is to treat the data with the same wavelength but at different temperatures in the same way as data at different times, thereby automatically requiring the linear coefficients, $\epsilon_i(\lambda)$ in Eq. 14, which are the spectra, to be the same for different temperatures. The data at additional temperatures are literally added in the time dimension of the data arrays.

The parameters that are varied in Eq. 14 to obtain the best fit to the data are the spectra $\boldsymbol{\epsilon}$ and the basic parameters required to describe the $\mathbf{K}(T)$ matrices as described at the end of section 3. For each iteration in the nonlinear least squares search the nonlinear functions $\mathbf{p}(t, T)$ are calculated from the $\mathbf{K}(T)$ matrix using the basic program described in the paragraph containing Eq. 5 in section 2. It is required to do this calculation at each iteration for N_T temperatures, and the partial derivatives must be done numerically which requires essentially N_K additional calculations at each temperature, so the analytic method of calculating $\mathbf{p}(t)$ described in section 2 helps to reduce cpu time. Also, the nonlinear least squares program that drives the search is the VARP program of Golub and Leveque (4). This program ingeniously reduces the dimensionality of the search space to the number of nonlinear variables and needs only consider the linear variables, the $\boldsymbol{\epsilon}$, as a linear least squares problem once at the end of the calculation. Because the number, $2N_K$, of nonlinear variables in the $\mathbf{K}$ matrices, is roughly equal to the number of linear variables, ns, the dimensionality of the parameter space is effectively halved. In practice, choosing the basic nonlinear variables to be the logarithms of the independent rate constants at the highest and lowest temperatures appears to work best, even though a more symmetrical alternative choice is the f_{ij} and ΔE_{ij} in Eq. 8.

A direct method to obtain the photocycle $\mathbf{K}$ from vibrational data for $\mathbf{p}(t)$ has some similarities to the preceding method for treating data in the visible. The basic parameters to be varied in nonlinear least squares fitting are the logarithms of the independent rate constants K_{ij} in the $\mathbf{K}$ matrix, so negativity of rates is prevented. For each iteration the nonlinear functions $\mathbf{p}(t)$ are calculated from $\mathbf{K}$, with detailed balance automatically incorporated, and compared to the measured $\mathbf{p}(t)$. The $p_i(t)$ may be treated in two different ways. The first way lists all the data for all t and i as one vector. This means that there is only one linear parameter in the fitting. The second way uses n vectors, one for each p_i,

with length equal to the number of times observed, and all the p_i are fit simultaneously the same as for the first way. This means that there are n linear parameters that may be used to rescale the concentrations if the original normalizations are incorrect.

It is also important theoretically to mention a second method of solution of the vibrational problem. This consists first in using the VARP program to obtain the **C** matrix and the **k*** in Eq. 4. Second, the basic Eq. 1 may be written as n^2 linear equations

$$k_j^* C_{ji} = \sum_{m=1,n} K_{im} C_{jm}, \qquad (15)$$

which may then be solved uniquely for the K_{im}. The defect in this method compared with the one in the preceding paragraph is that it does not easily permit inclusion of the detailed balance constraint or nonnegativity of the basic rates. Nevertheless, it is worth mentioning because it is easy to see from Eq. 15 that there are as many equations as unknowns. This emphasizes theoretically that the photocycle **K** is uniquely determined by the $\mathbf{p}(t)$. It is also important to emphasize, when comparing to the method for data in the visible, that this determination requires data at only one temperature.

5. EXAMPLES

It is important to test the new nonlinear least squares program on data whose kinetic model is known. Because the kinetic models for real systems such as bacteriorhodopsin are not known, it is necessary to turn to data generated analytically, using the program described in connection with Eq. 5. The most precise data are accurate to ~10 significant figures and will be called the noiseless or $\sigma_o = 0$ data. The data examined in this section come from models with $n = 3$ intermediates, which is the smallest n with all the essential features of complex kinetic models, such as having a dependent rate constant due to detailed balance. Noisy data are produced with an additive random Gaussian distribution with rms width σ_o. Also, in the case of vibrational data, all $p_i(t)$ smaller than σ_o are set equal to zero and no negative values are allowed.

A. Visible spectroscopy

The spectra of the three intermediates used to construct the data are shown in Fig. 2, but not all 10 wavelengths are used in each calculation.

First, consider a kinetic model, to be called M1, which has strong backreactions and no K_{ij} rate very small compared with the other ones. For the temperatures 300 and 280 K this model has the $\mathbf{K}(T)$ matrices shown in Table 1, where the K_{ij} is the rate for transition from state j (the column index) to state i (the row index). The last or $(n + 1)$st row consists of the rates K_{0j} due to branches straight to the final state. Visible absorption data for the M1 model at $T = 300$ K and for three wavelengths are shown in Fig. 3 for noiseless data and for data with 1%

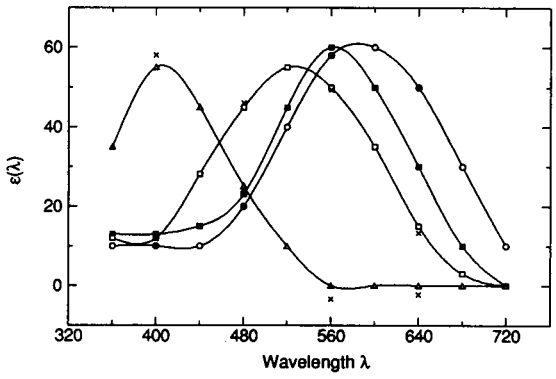

FIGURE 2 The spectra of the intermediates used in the examples in this paper. Intermediate 1 is indicated by open circles, intermediate 2 by open squares, intermediate 3 by open triangles, and the final state 0 is indicated by solid squares. The crosses at 400, 480, 560, and 640 nm show results to be described when fitting data with 0.1% noise.

TABLE 1 K matrices at two temperatures for the M1 model

$T = 300\,K$			$T = 280\,K$		
−11.500	10.000	1.000	−3.582	3.041	0.435
10.000	−15.000	4.000	3.041	−5.633	2.206
1.000	4.000	−7.000	0.435	2.206	−3.120
0.500	1.000	2.000	0.106	0.386	0.479

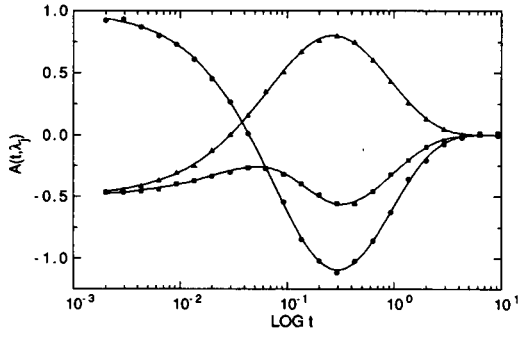

FIGURE 3 Visible absorption date for the M1 model for λ = 440 nm (*triangles*), 520 nm (*squares*), and 600 nm (*circles*) at $T = 300$ K. The noiseless data are shown by the smooth curves and the data with 1% noise ($\sigma_o = 0.01$) are shown by the solid symbols.

TABLE 2 **Result using two temperatures only**

Initial K-1			Final K		
−12.500	9.000	0.614	−12.136	9.858	0.984
11.000	−13.500	3.000	10.009	−14.674	3.891
1.000	4.000	−5.614	1.101	4.286	−6.688
0.500	0.500	2.000	1.026	0.530	1.813

TABLE 3 **Result using two temperatures only**

Initial K-2			Final K for two T's		
−13.000	9.000	0.375	−11.434	10.380	0.947
12.000	−13.000	3.000	9.662	−14.948	4.202
0.500	3.000	−5.475	0.830	3.955	−7.117
0.500	1.000	2.100	0.942	0.613	1.968

noise. Notice that the $A(t, \lambda)$ are of order unity because of the choice of scale for $\epsilon(\lambda)$ in Fig. 2.

Noiseless data from model M1 at $s = 10$ wavelengths were analyzed using only two temperatures, $T = 300$ and 260. The program successfully fit the data to high accuracy ($\sigma = 10^{-10}$). Table 2 shows the initial and final $\mathbf{K}(T_{300})$ for only one temperature. Although the final **K** is much closer to the true **K** in Table 1 than the initial **K**-1, it is distinctly different. Also, the spectra from this calculation differ noticeably from the true spectra. A similar example, but with a different initial **K** further from the true one is shown in Table 3. Again, the program successfully fits the data to high accuracy, but the final **K** and the spectra are different from the true **K** and also from the result when **K**-1 was the initial matrix. The results in Tables 2 and 3 are consistent with the theory in section 3 which states that with only two temperatures the problem is indeterminate with a local infinity of possible solutions which fit the data to within the very high precision of these data.

The same noiseless M1 data were fit using three temperatures, 300, 280, and 260 K, again with variable initial $\mathbf{K}(T)$. For either of the initial **K**-1 or **K**-2 shown in Tables 2 and 3 the program converged to the true solution in Table 1 for the **K** and the ϵ in ~10 cpu minutes on a microvax II. This supports the theoretical conclusion that three temperatures suffice to make the problem locally determinate. As the number of wavelengths included in the calculation was reduced from $s = 10$, the number of iterations in the nonlinear least squares fitting increased, but the cpu time per iteration decreased. For the initial conditions shown in the preceding two tables, the actual running time decreased steadily as s was reduced from 10 to 4. When s was reduced further to $s = 3$ the running time increased again, sometimes by a great deal. These results are in agreement with the analysis in the preceding section that only as many wavelengths as intermediates are required for local determinateness, but they also indicate that taking additional wavelengths facilitates the computational process.

An additional issue is whether the resulting rate constants and spectra are determined better with noisy data when more wavelengths are used than the theoretical minimum. Table 4 shows the errors for the rate constants. The data in column two consisted of a subset of four wavelengths from the data in column four and the noise in the data in column three was scaled by a factor of $SF = (10/4)^{**}0.5 = 1.58$ from the data in column four. If the same amount of total data were taken, then each data point from the set with 10 wavelengths would be SF times noisier than the set with four wavelengths. In this case the appropriate comparison is column two with column three, for which the errors are comparable. Even with data of equal accuracy at each data point, increasing s from 4 (column 2) to 10 (column 4) does not dramatically improve the estimation of the rates. Comparison of column 4 with column 3 shows that decreasing the noise decreases the errors, as expected.

The question of global determinateness was addressed by starting with initial **K** further from the true solution than **K**-1 or **K**-2. The following two initial **K**-3 and **K**-4 both converged to the same false final $\mathbf{K}_f$ shown in Table 5. This confirms that there are secondary minima in the nonlinear least squares function for this kind of problem. This secondary minimum fits the data with a σ of 0.00060. This is larger by seven orders of magnitude than the σ of the true solution. However, it corresponds to a signal-to-noise ratio of ~1,500, so the next issue to be addressed concerns the ability to

TABLE 4 **Relative errors in rate constants of the M1 model as a function of number of wavelengths S and noise conditions**

S	4	10	10	10	10
σ_0	0.001	0.00158	0.001	0.01 (tT)	0.01 (lT)
Rate					
1 → 2	−0.021	−0.015	−0.008	−0.021	−0.173
1 → 3	0.025	−0.034	−0.017	1.820	0.867
1 → 4	−0.100	−0.296	−0.194	13.754	−0.340
2 → 3	−0.014	−0.038	−0.022	0.553	−0.293
2 → 4	−0.037	0.203	0.126	−0.862	0.235
3 → 4	0.071	0.010	0.006	−0.975	0.163
2 → 1	0.027	0.009	0.004	−0.499	0.247
3 → 2	−0.031	0.017	0.010	−0.744	−0.415

The first column lists the independent transitions. The relative errors shown were determined by subtracting the true rate from the best fitted rate and then dividing by the true rate. The nature of the noise in the last two columns (five and six) is explained in the discussion.

TABLE 5 **Initial K's leading to false result**

K-3			K-4			False K-f		
−22.40	1.70	0.06	−15.00	3.00	0.06	−21.52	2.86	0.09
19.20	−9.20	1.50	13.00	−9.70	1.00	10.67	−9.69	1.20
2.70	6.50	−2.71	1.50	6.00	−2.06	1.65	6.09	−2.24
0.50	1.00	1.15	0.50	0.70	1.00	9.20	0.74	0.95

distinguish between the true solution and spurious solutions when there is noise in the data.

For all values of noise σ_o examined, the initial **K**-1 in Table 2 led to a final model close to the true model, with errors that grew larger with σ_o. (Numerical results will be deferred to Table 8 in section 5 *B*.) For all values of σ_o examined, the initial **K**-4 in Table 5 led to a final model that was very similar to the False **K**-f in Table 5, again with differences that grew with σ_o. For both cases the goodness of the fit was determined as measured by the average root mean square deviation σ of the fit (with $2N_K + N_T n^2$ subtracted from the number of data points to account for the number of constraints). Table 6 shows the results for σ_t, the solution close to the true solution, and for σ_f, the solution close to the false solution, as a function of the chosen noise level, σ_o. Table 6 shows that as the noise level σ_o exceeds the depth of the false minimum, it becomes more difficult to discriminate the true solution from the false one because the fits become quantitatively comparable. (It may also be noted that σ_t was distributed randomly about σ_o when a variety of different seeds was used in the random number generator that produced the noise.)

The effect of relaxing the constraint that the spectra of the intermediates are independent of the temperature was also investigated. The spectra of the intermediates at T = 300 K were uniformly increased by ~1% and they were decreased at T = 260 K by ~1% for an overall variation of 2%. The resulting best fit obtained by requiring the fitted model to have temperature invariant spectra yielded σ = 0.0053. The **K** and ϵ so obtained were comparably accurate to results obtained when a comparable amount of noise was added.

All the rate constants in the M1 model are nonzero.

TABLE 6 **Comparison of goodness of fit of true and false solutions**

Noise	True	False
σ_o	σ_t	σ_f
0	10^{-10}	0.00060
0.0001	0.00011	0.00063
0.0005	0.00054	0.00084
0.001	0.00108	0.00124
0.002	0.00216	0.00223

TABLE 7 **The M2 model and an initial guess**

True K			K-5		
−10.00	1.90	0	−12.20	0.10	0.00
10.00	−2.90	0.19	12.00	−1.15	0.01
0	1.00	−0.29	0.10	1.04	−0.90
0	0	0.10	0.10	0.01	0.08

Next, consider a model, M2, with no branches, with $\mathbf{K}(T_1)$ shown as the first matrix in Table 7. The second matrix in the table shows an initial guess, K-5. This initial guess was based on a unidirectional unbranched model, so the matrix elements $K_{i+1,i}$ were chosen close to the apparent rate constants. The other matrix elements were all chosen to be small but not zero because that would make the derivative matrix in the nonlinear least squares program singular. Starting from K-5 the program did not converge, but it consistently pushed K_{41} to much smaller values, suggesting that this branch should be eliminated. The program was modified so that any set of the original K_{ij} could be eliminated, thereby reducing the number of nonlinear parameters. In the next calculation with K_{41} eliminated, the program drove K_{42} to much smaller values. The process was repeated with both K_{41} and K_{42} set to zero, and the calculation then drove K_{31} to much smaller values. Finally, eliminating all three branches ($K_{31} = K_{41} = K_{42} = 0$) resulted in rapid convergence to the true model with backreactions ($K_{12} \neq 0$ and $K_{23} \neq 0$).

B. Vibrational spectroscopy

For comparison with the visible spectroscopy results, results for the M1 model will also be given for the vibrational spectroscopy solution. The data for T = 300 K consist of the $p_i(t)$. These are shown in Fig. 4 for noiseless data and for data with σ_o = 0.01. Because the

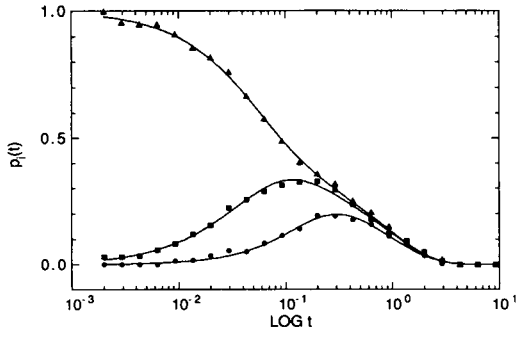

FIGURE 4 The concentrations $p_i(t)$ of the intermediates, i = 1, 2, 3, vs. LOG_{10} of the time. The solid curves show the noiseless $p_i(t)$ and the solid symbols show $p_i(t)$ for 1% noise, σ_o = 0.01.

intermediates are strongly coupled by backreactions, the final decays of all three intermediates are governed by the smallest apparent rate constant.

The great simplicity in the results for **K** matrices from vibrational spectroscopy compared with visible spectroscopy is that they appear to be globally unique. Using the first method for the vibrational problem described in section 4 and starting from either the initial **K**-1 in Table 2, the initial **K**-2 in Table 3 or the initial **K**-3 or **K**-4 in Table 5 yields the exact **K** shown in Table 1 when noiseless data are examined. The same exact result is also obtained using the second method for the vibrational problem described in section 4 when the VARP program is given reasonable estimates of the apparent rate constants, obtained, for example, by simple graphical methods (10). The first program takes about half a minute cpu time on a microvax and the second program runs even more quickly.

The results for the **K** matrices when noise is added to the vibrational data are shown on the left-hand side of Table 8 when the first method is used. The **K** matrices obtained when noise is added to the $\mathbf{p}(t)$ are the best solutions when the detailed balance and nonnegativity constraints are imposed, and the $\mathbf{p}(t)$ calculated from these **K** matrices agree with the initial data to within the known noise level. When the second method of computation was employed, the fits were slightly better and the final **K** matrices violated the physical criteria of detailed balance and nonnegativity; both differences would be expected since the corresponding constraints were not imposed upon the fit.

As can be seen by comparison with the noiseless **K** matrix at the top of Table 8, increasing noise leads to larger errors in the determination of the true rate constants. Finally, for convenient comparison in the discussion, the **K** matrices obtained from the visible spectroscopic data with the same level of noise are shown on the right-hand side of Table 8.

TABLE 8 Results for *K*'s for vibrational data and data in the visible

σ_0	*K*-Vibrational			*K*-Visible		
	−11.50	10.00	1.00	−11.50	10.00	1.00
0	10.00	−15.00	4.00	10.00	−15.00	4.00
	1.00	4.00	−7.00	1.00	4.00	−7.00
	0.50	1.00	2.00	0.50	1.00	2.00
	−11.56	10.08	1.08	−10.99	10.62	1.12
0.002	9.94	−14.82	3.84	9.50	−15.38	3.72
	1.07	3.85	−6.96	1.05	3.89	−7.16
	0.55	0.89	2.05	0.43	0.87	2.32
	−11.96	10.64	1.45	−8.20	14.55	1.91
0.015	9.55	−13.62	2.62	6.43	−17.74	1.74
	1.48	2.98	−6.71	1.55	3.19	−7.68
	0.94	0.00	2.64	0.22	0.00	4.02

6. DISCUSSION

A. Visible spectroscopy

In general a unique description of the kinetics of spectroscopic data in the visible for systems with broad absorption bands is impossible unless there are constraints. The constraint utilized in this paper is that the spectrum relative to the initial bR state of each intermediate is invariant with temperature. While there may be exceptions, such as when the temperature is dropped very low or when the configuration of a protein undergoes a structural phase transition with temperature, this constraint would seem to be an appropriate one whenever the concept of a chemical intermediate is appropriate. An apparent exception would be if there were a fast equilibrium between two intermediates with different spectra which would be difficult to distinguish from one intermediate with a composite spectrum that would vary with the temperature dependence of the fast equilibrium; such an exception can easily be treated by an extension of the methods in this paper. The results of imposing this constraint upon data which violated it were investigated. Roughly, $p\%$ variations in the spectra were equivalent to adding $\sim 0.3p\%$ noise to the data.

The most important theoretical result in this paper concerns the kind of data in the visible required to allow for a unique description of the bR photocycle. This paper proves conclusively that it is necessary to make measurements at three temperatures at least. Fortunately, the number three is independent of whether there is or is not an Arrhenius type relation, so this issue need not be resolved before obtaining data. Of course, if data at additional temperatures were available, they could then be used in the fitting or they could be used to check the result obtained from the other three temperatures.

The reason that two temperatures do not suffice is that there are only n linearly independent spectra when there are n intermediates. This in turn means that doing measurements at more than n linearly independent wavelengths is theoretically redundant for obtaining the basic kinetics, and this was verified by explicit computations for examples without noise and with noise (compare columns two and three in Table 4). This strong statement is softened somewhat by the observation in this paper that an actual calculation may proceed most rapidly when $n + m$ wavelengths are included, where, in the examples in this paper, m equals one. There are also other reasons to include more than the minimum number of wavelengths in experiments. The preliminary step

of determining the number of intermediates n may require more than n wavelengths, as in the work of reference 18 where $s = 15$ wavelengths were measured, even though there were only $n = 7$ intermediates. Furthermore, it is desirable to have enough wavelengths to be able to interpolate to reliable continuous spectra after the K-matrices are obtained.

As would be expected, the results for the K-matrix and the ϵ are better when noisy data taken at more rather than fewer wavelengths are analyzed simply because there are more data points, each with equal noise, as can be seen by comparing column four of Table 4 with columns three and two. Therefore, if one has data at a larger number of wavelengths than the theoretical minimum, it makes sense to use them in the analysis. The more interesting question concerns optimal design of apparatus to solve the kinetics of photocycles. The next three paragraphs discuss two designs in current use.

The first design (6, 17) measures many wavelengths simultaneously by using a measuring beam which consists of white light. The measuring beam is flashed or gated so that its broad spectrum is not actinic. Although this design yields data with little noise from wavelength to wavelength at the same time in the photocycle, the experiment must be repeated for each measuring time, so there is substantial noise from time to time. Column five in Table 4 shows that fitting data with 1% noise just along the time direction and not along the wavelength direction gives very poor results for the rate constants; in fact, the results are as poor as for general 1% noise in both the time and wavelength directions.

In the second design (18) data are taken with a fast detector using a measuring beam that is on during the entire photocycle and which is made weak to minimize actinic effects by filtering to a small wavelength range. This yields data one wavelength at a time with small errors along the time direction but with larger errors (of order 1%) in the wavelength direction. With data that have small noise (say 0.1%) in the time direction, but larger noise (say 1%) in the wavelength direction, the results for the rate constants are independent of the latter larger noise; only the spectra are incorrect at the 1% level. This suggests that the second equipment design is superior to the first design for the purpose of determining the K-matrix which is the necessary prerequisite for obtaining the spectra of the intermediates.

There is, however, a problem with the second design, because there is also noise between measurements at different temperatures, even at the same wavelength. (Such noise also occurs for the first design, and was included in column five of Table 4). The result of fitting data with 1% noise in the wavelength and the temperature directions is shown in the last column (six) of Table 4. While these results are better than the results in column five, the errors are still unacceptably large. One way to solve this problem is to eliminate the wavelength errors in data taken using the second design by normalizing these data at all times to data taken at one (or a few) delay times using the first design. This still leaves noise between different temperatures, but this has been easily accommodated in the fitting program described in this paper by adding one scale factor for each temperature. These scale factors are required in any case because the fraction cycling may be different at different temperatures, and one may see from the formulae developed in section 3 that they do not affect local uniqueness of the solutions. Another way to solve this problem is to use a scale factor for each wavelength at each temperature; while this requires more ($N_T s$) scale factors, local uniqueness can still be guaranteed. The VARP driver program does not allow for this option, but other driver programs do (R. H. Lozier, manuscript in preparation). In contrast, the number of scale factors that would be required to eliminate the noise in the time direction for data taken using the first design is too large for local uniqueness because there would have to be a scale factor for each of at least 40 times and three temperatures.

In general, for nonlinear problems, there may be several different descriptions that fit the data equally well; such degeneracy may be classified into local vs. global degeneracy. Local degeneracy of the fundamentally linear kind is removed by requiring that the number of parameters describing the data exceeds the number of parameters to describe the solution; in this paper this is guaranteed by having data at three or more temperatures. One could also conceivably have accidental local degeneracy of a nonlinear kind, such as occurs when the activation energies are equal for all the rate constants, but this is not a general occurrence. Degeneracy may also be nonlocal, i.e., global. In this case there are different solutions, each of which is locally the best one. It is appropriate to distinguish two types. The first type is true degeneracy, in which noiseless data could be fit with no error by two different kinetic descriptions. There is no way to resolve true degeneracy, but no examples of this have been found in this work. The second type of global degeneracy consists of a true solution, which fits noiseless data perfectly with $\sigma_t = 0$, and a false solution, which is locally the best solution but which does not fit noiseless data perfectly, $\sigma_f > 0$. This type of global degeneracy becomes difficult to distinguish from the first type when the data contain noise, $\sigma_o > 0$, especially when σ_o sufficiently exceeds σ_f, as was illustrated by Table 6 for the main example in this paper. This kind of degeneracy is, however, resolvable in principle by obtaining better data with a noise level $\sigma_o \leq \sigma_f$.

When deciding what kind of data to take, the need to improve the noise level to remove global degeneracies

should be coupled to the result that more than n wavelengths are redundant. From the results in this paper there is a clear preference to concentrating on high precision data, especially in the time dimension, at fewer wavelengths, than to measuring many wavelengths with less precision.

The principle methodological advance in this paper for treating spectroscopic data whose intermediates have broad overlapping bands is the description and implementation of a direct method to obtain locally unique kinetic descriptions from data. This method organizes data in a way to impose temperature invariance of the spectra, it uses fast Laplace transform methods for calculation of the kinetics, and it uses the nonlinear least squares VARP driver program (4) which eliminates the linear spectral variables from the search. Instead of building up from less general to more general kinetic models, this method starts with the most general model where all possible transitions between intermediates are allowed. When appropriate, it works down in a systematic way to less general models with some rate constants set to zero. This seems, in principle, to be less prone to missing the best kinetic description. However, as with any method, initial models to start the calculation must sample enough of the possible solution space not to miss the best solution. Nevertheless, this method provides a larger and more systematic searchlight for finding the best kinetic description to spectroscopic photocycles.

B. Vibrational spectroscopy and comparison to visible spectroscopy

The problem of extracting the kinetic model embodied by the **K** matrix is relatively straightforward when the $\mathbf{p}(t)$ are measured directly. There is no need to consider more than one temperature and the method of solution is virtually free of the problem of false solutions or of having to consider many possible starting values in the computer programs. These features give the vibrational approach a clear advantage over the visible approach to such problems.

As may be seen in Table 8, the numerical results for the **K** are quite good when the noise level is $\sigma_o = 0.002$. As the noise level is raised to $\sigma_o = 0.015$, however, qualitatively incorrect conclusions can be drawn, such as the absence of a branch from the second intermediate to the final state (small K_{42} in the table). Nevertheless, the accuracy of the **K** results is comparable or perhaps even slightly superior to the accuracy obtained from data in the visible with the same noise level, as can be seen by comparing the results in Table 8.

The lowest noise level obtained so far for visible spectroscopic bR data (18) has σ_o near 0.002 when normalized according to the convention followed in this paper. From Table 8 such a low noise level yields reasonable values of **K** for the true solution. However, this noise level is large enough that it may be difficult to distinguish the true solution from false solutions, as indicated in Table 6.

The noise level obtained from the most accurate vibrational data (1) is presently ~ 0.015 or nearly 10 times poorer than for data in the visible. The above discussion regarding Table 8 suggests that the resulting **K** would be less accurate than that obtained from data in the visible and that it might even be qualitatively incorrect.

For the M1 model focussed on in this paper, there appears to be an obvious advantage to using both visible and vibrational spectroscopy. The **K** obtained in Table 8 from vibrational data with $\sigma_o = 0.015$ is much closer to the **K** obtained in Table 8 from data in the visible with $\sigma_o = 0.002$ than it is to the false solution in Table 5. This suggests that the vibrational result, which does not suffer from the nonuniqueness problem, may be used to discriminate between the more accurate, but multiple, solutions obtained from data in the visible. Also, the less accurate vibrational result, which can be obtained much more easily computationally with little ambiguity regarding starting values, can then provide good starting values for the calculations of **K** from data in the visible.

I wish to acknowledge very helpful discussions with G. H. Golub and M. Overton regarding the nonlinear least squares problem, R. W. Zwanzig regarding detailed balance, much exchange of information with R. H. Lozier who is tackling the bacteriorhodopsin photocycle along similar lines but with distinct differences, general discussions with W. Stoeckenius, and a preprint of reference 1 from R. A. Mathies.

Support for this work was obtained under grant GM40740 from the National Institutes of Health.

Received for publication 29 May 1990 and in final form 18 September 1990.

REFERENCES

1. Ames, J. B., and R. A. Mathies. 1990. The role of backreactions and protonation during the N → O transitions in bacteriorhodopsin's photocycle: a kinetic resonance raman study. *Biochemistry.* 29:7181–7190.
2. Beach, J. M., and R. S. Fager. 1985. Evidence for branching in the photocycle of bacteriorhodopsin and concentration changes of late intermediate forms. *Photochem. Photobiol.* 41:557–562.
3. Johnson, F. H., H. Eyring, and M. J. Polissar. 1954. The Kinetic Basis of Molecular Biology. John Wiley & Sons, Inc., New York. 874 pp.
4. Golub, G. H., and R. J. Leveque. 1979. Extensions and uses of the variable projection algorithm for solving nonlinear least squares

problems. *Proc. Army Numerical Analysis and Computing Conference, ARO Report.* 79–3:1–12.

5. Groma, G. I., and Zs. Dancshazy. 1986. How many M forms are there in the bacteriorhodopsin photocycle? *Biophys. J.* 50:357–366.
6. Hofrichter, J., E. R. Henry, and R. H. Lozier. 1989. The photocycle of bacteriorhodopsin in light- and dark-adapted purple membrane studied by time-resolved absorption spectroscopy. *Biophys. J.* 56:693–706.
7. Kouyama, T., A. Nasuda-Kouyama, A. Ikegami, M. K. Mathew, and W. Stoeckenius. 1988. Bacteriorhodopsin photoreaction: identification of a long-lived intermediate N(P,R-350) at high pH and its M-like photoproduct. *Biochemistry.* 27:5885–5863.
8. Lozier, R. H., R. A. Bogomolni, and W. Stoeckenius. 1975. Bacteriorhodopsin: a light-driven proton pump in halobacterium halobium *Biophys. J.* 15:955–962.
9. Maurer, R., J. Vogel, and S. Schneider. 1987. Analysis of flash photolysis data by a global fit with multi-exponentials I. and II. *Photochem. Photobiol.* 46:247–262.
10. Nagle, J. F. 1981. Upon the optimal graphical representation of flash data from photochemical systems obeying first order kinetics. *Photochem. Photobiol.* 33:937–939.
11. Nagle, J. F., L. A. Parodi, and R. H. Lozier. 1982. Procedure for testing kinetic models of the photocycle of bacteriorhodopsin. *Biophys. J.* 38:161–174.
12. Onsager, L. 1931. Reciprocal relations in irreversible processes. *Phys. Rev.* 37:405–426.
13. Parodi, L. A., R. H. Lozier, S. M. Bhattacharjee, and J. F. Nagle. 1984. Testing kinetic models for the bacteriorhodopsin photocycle-II. Inclusion of an O to M backreaction. *Photochem. Photobiol.* 40:501–512.
14. Rayfield, G. W. 1983. Events in proton pumping by bacteriorhodopsin. *Biophys. J.* 41:109–117.
15. Roepe, P., P. L. Ahl, S. K. Das Gupta, J. Herzfeld, and K. J. Rothschild. 1987. Tyrosine and carboxyl protonation changes in the bacteriorhodopsin photocycle. *Biochemistry.* 26:6696–6707.
16. Sherman, W. V., R. R. Eicke, S. R. Stafford, and F. M. Wasacz. 1979. Branching in the bacteriorhodopsin photochemical cycle. *Photochem. Photobiol.* 30:727–729.
17. Varo, G., A. Duschl, and J. K. Lanyi. 1990. Interconversions of the M, N, and O intermediates in the bacteriorhodopsin photocycle. *Biochemistry.* 29:3798–3804.
18. Xie, A. H., J. F. Nagle, and R. H. Lozier. 1987. Flash spectroscopy of purple membrane. *Biophys. J.* 51:627–635.